Adsorptive Separations Using Supercritical Frontal Analysis Chromatography

William M. Cross, Jr. and Aydin Akgerman
Chemical Engineering Dept., Texas A&M University, College Station, TX 77843

Many food products and pharmaceuticals industries are looking to integrating supercritical extraction and separations processes to fulfill processing needs due to limitations and regulations concerning the use of organic solvents. One such technology, which may affect these industries, is continuous supercritical adsorptive separation, a processing technology similar to the separation process of xylenes developed at UOP. Many products like pharmaceuticals and other human consumables could be processed more economically and with higher purity by supercritical fluid adsorption/desorption processes. Past studies, however, have focused on single-component adsorption/desorption involving a supercritical mobile phase, whereas adsorptive separations involving supercritical fluids are multicomponent systems. Accurate experimental techniques, which can determine both multicomponent solubilities in supercritical fluids and multicomponent adsorption isotherms in the presence of supercritical fluids, were developed to investigate the multicomponent supercritical adsorption phenomenon. A dynamic column model developed takes into account column dispersion as well as mass transfer and diffusive resistances. Experimental isotherm data incorporated into the model can predict the breakthrough profiles. An extension of pulse chromatography was used to identify the important hydrodynamic and transport parameters, and operating conditions are identified for optimal separations.

Introduction

Recently, separation technologies using supercritical fluids as the solvent medium have seen increasing use (Bruno and Ely, 1991). Some new technologies have been commercialized in applications such as decaffeination, natural products extraction, extraction of foodstuffs, supercritical chromatography and asphaltene processing, among others. Of particular interest with respect to the use of supercritical fluids is the separation of high value, low vapor pressure organic compounds. In addition to being able to handle separation of heavy molecular weight compounds, supercritical fluid chromatographic methods have shown promise for separation of structurally similar chemicals and isomers as well. An emerging technology in this regard, which may prove lucrative for the separation of structurally similar products such as pharmaceuticals, is adsorptive separations using supercritical fluids.

Correspondence concerning this article should be addressed to A. Akgerman.

Considerable research has been performed in the area of supercritical chromatography since the early 1980s. In addition, some experimental work on continuous separation of binary mixtures, such as indole from crude methylnaphthalene-based oil using ion-exchange resin (Sakanishi et al., 1996) and separation of 2,6- and 2,7-dimethyl naphthalenes via NaY zeolite (Uchida et al., 1997) have also been published. Previously, Lin and Tan (1991) reported on the pulse separation of *m*-xylene and ethylbenzene dissolved in high-pressure gaseous carbon dioxide using a silicalite adsorbent. Similarly, Tan and Tsay (1990) studied separation of xylene isomers in both gaseous and supercritical carbon dioxide. Studies have been published on supercritical desorption of single and multicomponent component organics from contaminated soil. In addition, adsorption isotherms are available for single component adsorption onto carbon, soil, and alumina in the presence of a supercritical fluid (Erkey et al., 1993; Madras et al., 1993, 1994; Macnaughton and Foster, 1995).

The majority of research involving supercritical fluid chromatography has concentrated on proper stationary phase development and determination of optimum conditions for chromatographic peak resolution, without going into detailed analysis of the thermodynamics and the kinetics of the chromatographic separation process itself. Adsorptive separation technology, on the other hand, makes use of the information generated on suitable stationary phase development (adsorbents) but necessitates a thorough understanding of the thermodynamics and kinetics of the process for scale-up purposes. Currently, no quantitative analysis of a supercritical frontal chromatography system for separation and its mathematical modeling is available.

In the envisioned process, the two chemicals to be separated are dissolved in a supercritical solvent, such as carbon dioxide, and passed over a packed-bed adsorption column. The desired compound is either concentrated in the column by adsorbing on the adsorbent or concentrated in the effluent. The adsorbent would then be regenerated by the pure solvent. The technique, called frontal analysis chromatography, is a separation technique based on different adsorptive interactions of the species with the adsorbent combined with adsorption column hydrodynamics and mass-transfer characteristics. The system consists of an adsorbent material (solid phase), the supercritical fluid (mobile phase), and components A and B (solutes) which are partitioning between the two phases.

Figure 1a illustrates typical breakthrough profiles for a binary mixture of A and B, where B is the component adsorbing strongly. The ordinate is the normalized concentration of each species (effluent concentration divided by inlet concentration) and the abscissa is time. The portions of the first curve which move above the normalized concentration of 1.0 are referred to as the roll-up portion, providing an outlet concentration higher than the inlet. This is a common phenomenon in multicomponent adsorption. Once the breakthroughs are established, the amount of A adsorbed on the column is area I minus area II, whereas the amount of B adsorbed is area I plus area III. The residence time for each species is t_a and t_b, respectively. The residence time is determined solely by the adsorptive strength of each species, that is, the adsorption isotherm of each species in the presence of each other at the given concentration level in supercritical fluid. The steepness of the profiles, on the other hand, is determined by the mass-transfer characteristics of each species combined with the column hydrodynamics. If a suitable adsorbent is operated at conditions as shown in Figure 1b, such that area I is approximately equal to area II, the adsorbed species on the column will be essentially pure B, in effect the desired component B is separated from A and concentrated in the adsorption column. Normally, the column is then regenerated by the pure solvent (or another suitable solvent) and the expansion of the supercritical fluid yields pure B. At the mean time, the effluent from the column contains pure A in the time period t_1 to t_2. By orienting the process in this fashion, operating conditions can be determined for a more suitable industrial process, such as a moving bed process.

This adsorptive separation process involves multicomponent adsorption/desorption phenomena. Although adsorption-based separation is an established technology for gas

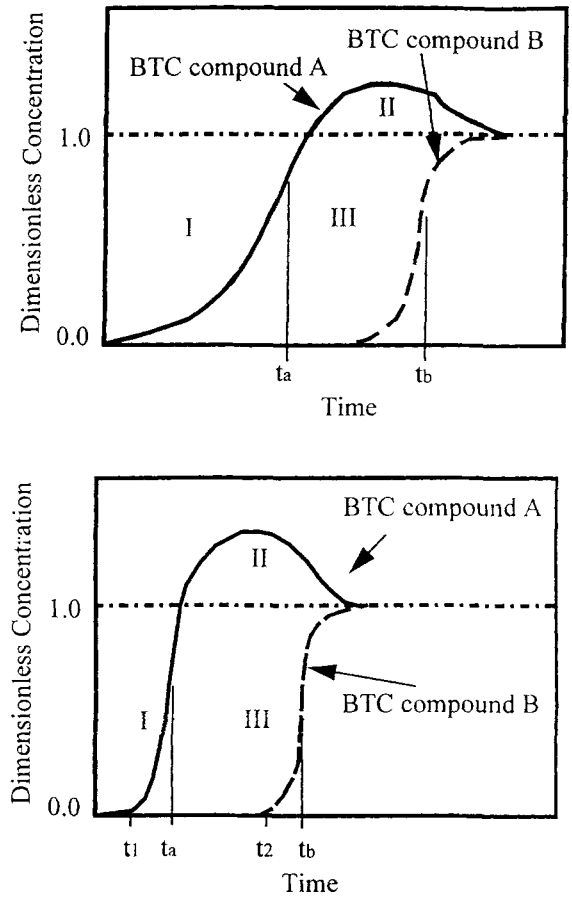

Figure 1. Binary breakthrough profiles: (a) typical breakthrough; (b) optimized breakthrough.

separation and purification, that is, pressure and/or temperature swing adsorption (Ruthven, 1984), the fundamentals related to multicomponent adsorption from supercritical fluids are yet to be developed. This study focuses on developing a fundamental understanding of adsorptive separations employing supercritical fluid mobile phases with three primary objectives: (1) development of the experimental techniques required to determine multicomponent adsorption isotherms in the presence of supercritical fluids and multicomponent solubilities in supercritical fluids; (2) development of theoretical models for prediction of multicomponent adsorption column breakthrough curves and multicomponent solubilities; and (3) development of methodology for determination of optimum operating conditions for supercritical fluid adsorption processes.

Theoretical Model Development

The mass balance equations for a supercritical adsorber operating under isothermal and isobaric conditions are given by Eqs. 1–7 in cylindrical coordinates

$$\frac{\partial C_i}{\partial \tau} - \frac{1}{Pe_B}\frac{\partial^2 C_i}{\partial z^2} + \frac{\partial C_i}{\partial z} + \frac{1-\epsilon_B}{\epsilon_B}\frac{3L}{R_p}\frac{Bi_i}{Pe_{P_i}}(C_i - C_i^s) = 0 \tag{1}$$

$$\frac{\partial C_i}{\partial z} = Pe_B\left(C_i - C_i^0\right) \quad \text{at} \quad z = 0;$$
$$\frac{\partial C_i}{\partial z} = 0 \quad \text{at} \quad z = 1 \tag{2}$$

$$\left[\epsilon_p \frac{\partial C_{P_i}}{\partial \tau} + (1-\epsilon_P)\frac{\partial q_i}{\partial \tau}\right] = \frac{1}{Pe_{P_i}}\frac{L}{R_p}\frac{1}{\rho^2}\frac{\partial}{\partial \rho}\left[\rho^2 \frac{\partial C_{P_i}}{\partial \rho}\right] \tag{3}$$

$$\frac{\partial q_i}{\partial \tau} = \sum_{j=1}^{n}\left(\frac{\partial q_i}{\partial C_{P_j}}\right)\left(\frac{\partial C_{P_j}}{\partial \tau}\right); \quad q_i = \frac{a_i C_{P_i}}{1 + b_i C_{P_i} + \sum_{j \neq 1} b_j C_{P_j}} \tag{4}$$

$$Bi_i\left(C_i - C_i^S\right) = \frac{\partial C_{P_i}}{\partial \rho} \quad \text{at} \quad \rho = 1;$$
$$\frac{\partial C_{P_i}}{\partial \rho} = 0, \ \frac{\partial q_i}{\partial \rho} = 0 \quad \text{at} \quad \rho = 0 \tag{5}$$

At $\tau = 0$, $C_i = 0$ $C_{P_i} = 0$ $q_i = 0$

[for Adsorption] (6)

At $\tau = 0$, $C_i = C_i^0$ $C_{P_i} = C_i^0$ $q_i = q_i^0 = f\left(C_i^0\right)$

[for Desorption] (7)

Equations 1 and 2 define material balance for the mobile phase (supercritical phase), whereas Eqs. 3 and 5 define mass balance in the stationary phase. As shown in Eq. 2, the Danckwerts' boundary condition is used at the adsorber inlet for the fluid phase with the initial condition being that of a step change, or a front, at time zero. An empirical Langmuir or Markham-Benton multicomponent adsorption isotherm equation is used as given by Eq. 4. Use of this type of an isotherm has worked well in describing roll-up effects shown in Figure 1 for many gaseous adsorption models (Santacesaria et al., 1982). Equations 6 and 7 are the initial conditions for adsorption and desorption, respectively, that is, Eq. 6 applies for adsorption and Eq. 7 for column regeneration. For this relatively simple multicomponent system with only two adsorbing species and an inert carrier, the resulting mathematical expression involves four coupled partial differential equations.

Several key physical properties and hydrodynamic, mass transfer, and thermodynamic parameters are required to define the system and solve the model equations above. (1) Adsorbent particles' average size and particle-size distribution, particle porosity, and bed void fraction; (2) inlet concentrations C_i^0 (mol/m^3) (expressed as percentage of the solubility) of the individual solute species in the supercritical fluid in presence of each other; (3) the multicomponent adsorption isotherms; (4) the effective diffusivities of the individual species in presence of each other; (5) the supercritical fluid/solid mass-transfer coefficient of each species; and (6) the column axial dispersion coefficient.

Until the early 1990s, correlations were not available for prediction of the mass-transfer and hydrodynamic parameters. Some recent correlations are now available for mass transfer (Lee and Holder, 1995), dispersion (Catchpole et al., 1996), and molecular diffusion (Eaton and Akgerman, 1997) to obtain good estimates of the Peclet and the Biot numbers in the supercritical fluid for use with fixed-bed adsorbers and reactors. The only remaining variables which require direct measurement are the particle properties, bed voidage, and the thermodynamics of the mixture, that is, multicomponent solubilities (the feed stream composition entering the adsorber) and the multicomponent adsorption isotherms. Of particular interest is the accurate measurement of the isotherms since these control the column breakthrough. To the best of our knowledge, there are no data on multicomponent adsorption isotherms in supercritical fluids, primarily due to the difficulty associated with their measurement.

The dynamics of the multicomponent separation process (Eqs. 1–7) are solved numerically by using the method of collocation on finite elements to break down the partial differential equations into a set of algebraic differential equations (ADEs). The ADEs are then solved at small incremental time steps given by a backward difference method much like that of previous adsorption modeling work on liquid and gas adsorption (Yu and Wang, 1989). The initial condition of a step change or front at time zero is introduced by the application of Eq. 8 into the computer code

$$C_{in} = C_o - C_o \exp[-1 \times 10^{10} \tau] \tag{8}$$

To ensure convergence in the numerical solution, the number of elements and collocation points for the column and particle are increased while the initial time step is decreased for each breakthrough curve considered. When the number of elements, number of collocation points in both the radial and axial direction, and initial time step no longer affected the shape of the breakthrough curve, the simulation was considered to have converged to the actual solution. The details and the computer code are available elsewhere (Cross, 1997).

Model System, Adsorbent Material and Properties

The model system studied was separation of hexachlorobenzene (HCB) and pentachlorophenol (PCP) since single component adsorption/desorption data had been previously determined for these compounds (Erkey et al., 1993; Madras et al., 1993, 1994). For the structurally similar HCB/PCP model separation, the adsorbent needs to interact with the slightly polar component since the only difference structurally between the two solutes was that of the -OH group on the PCP molecule. Natural zeolitic clay materials, which are Lewis acids, would be appropriate for the separation. For this study, Ca^{+2} Montmorillonite was chosen. Interaction between the Ca^{+2} cation/H_2O interlayer and the -OH group on the PCP molecules is believed to cause the separation of the two components, which is verified by pulse chromatography (Figure 2).

The average pore diameter of the solid adsorbent was determined as 75.8 Å by nitrogen adsorption. The pillared spacing between layers of the Ca^{+2} Montmorillonite was 15.15 Å, as determined by X-ray diffraction analysis. For modeling purposes, the smaller of the two pores, the interlayer spacing, was used to determine the controlling diffusional resistance. The measured pore volume was 0.24 cm^3/g. The solid density was measured as 1.88 g/cm^3 using a pycnometer. These values

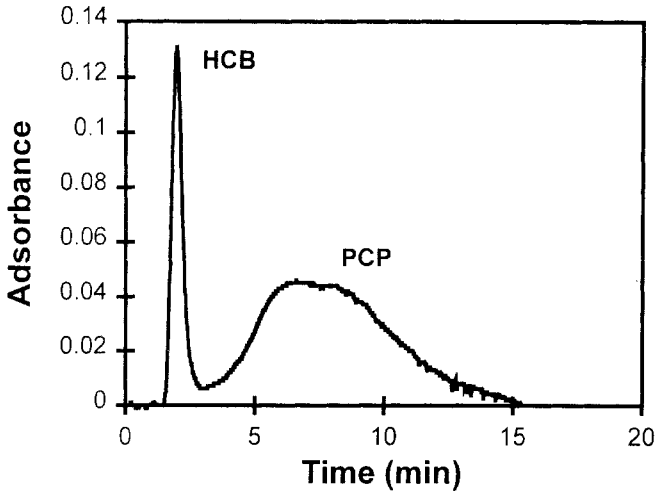

Figure 2. Pulse chromatography separation of HCB and PCP in supercritical carbon dioxide.

yield a particle porosity of 0.31. Bed porosity was calculated to be 0.47 using the measured total volume of the column, mass of adsorbent loaded, and density of the particles.

Particle-size distribution was determined using a pipette technique (Cross, 1997). The distribution was fit using a three parameter equation (Eq. 9) similar to that of a Rosin-Rammler distribution function traditionally used to describe particle-size distributions (Svarovsky, 1990). The average diameter of the particles was determined to be 5 microns for the montmorillonite clay by determining the mean length using Eqs. 10 and 11:

$$F(x) = \left[1 - \left(\frac{x}{x_0}\right)^S\right]^R \tag{9}$$

$$f(x) = -\frac{dF(x)}{dx} \tag{10}$$

$$\bar{X} = \int_0^1 x f(x) dx \tag{11}$$

In these equations $F(x)$ is the percent undersize, x is the particle size, and x_0, S and R are the fitted parameters.

Solubility and Adsorption Isotherm Measurement

The inlet concentrations of the species fed to the column are controlled by the mixture solubilities of the two components in the supercritical fluid at the column conditions. The determination of mixture solubilities of heavy molecular weight nonvolatile species has been considerably difficult and often inaccurate until recently. In most experimental equipment used for supercritical fluid equilibria, the dissolved heavy molecular weight components are precipitated out upon expansion of the supercritical fluid, causing loss of material within the pressure regulating device (such as a restrictor or a back pressure regulator). Precipitation of the material within the pressure regulator also introduces pressure increases in the equilibrium chamber due to clogging. Such pressure increases, although sometimes small and insignificant for solubility measurements, do cause considerable error for dynamic, multicomponent adsorption isotherm measurements where runs are of much longer duration and accurate data of the breakthrough profiles are required.

To alleviate such errors and allow for multicomponent adsorption studies, we developed a new technique where the supercritical fluid is mixed with an organic solvent before expansion (Cross et al., 1996; Cross and Akgerman, 1997). This technique of mixing the supercritical fluid with an organic solvent before expansion minimizes the errors in solute concentration measurement and eliminates the problems associated with clogging due to solute crystallization and pressure increases. Thus, during the expansion, the supercritical fluid and the organic solvent form a two-phase system and the solute that crystallizes out of the supercritical phase dissolves in the organic phase. The equipment is used to measure multicomponent solid solubilities, as well as multicomponent adsorption isotherms of pentachlorophenol and hexachlorobenzene in the presence of supercritical carbon dioxide. The mixture solubilities (the maximum adsorption column inlet concentrations) are summarized in Table 1. The details of the solubility determinations are given elsewhere (Cross and Akgerman, 1997).

The procedure was slightly modified for measurement of the adsorption isotherms and the multicomponent breakthrough curves by incorporation of an additional syringe pump for dilution of the saturated supercritical stream and the packed-bed adsorption column as shown in Figure 3. We have previously used a UV detector for continuous monitoring of the adsorption breakthroughs for single component systems (Cross et al., 1996; Erkey et al., 1993). For multicomponent measurements, the task becomes more involved, since additional components cause signal interference between the individual component's UV absorbance. In these cases, the UV detector serves only in a qualitative manner to determine when the breakthrough starts and when sampling should begin and end. The measurement of the individual component concentrations takes place at the liquid/gas separator by taking mixing cup readings of the solvent (alcohol) stream. The

Table 1. Mixture Solubilities of PCP and HCB in Supercritical Carbon Dioxide

T K	P bar	Density (g/cm^3)	PCP (mol fraction)	±	HCB (mol fraction)	±
308	90.0	0.6537	1.03×10^{-4}	7.10×10^{-6}	2.04×10^{-5}	3.78×10^{-6}
308	96.7	0.7027	1.27×10^{-4}	1.05×10^{-6}	2.24×10^{-5}	2.74×10^{-6}
308	112.4	0.7470	1.49×10^{-4}	6.46×10^{-6}	2.34×10^{-5}	3.14×10^{-7}
308	136.5	0.7941	1.91×10^{-4}	6.26×10^{-6}	2.78×10^{-5}	2.04×10^{-7}
308	186.2	0.8520	2.46×10^{-4}	7.66×10^{-6}	3.42×10^{-5}	1.26×10^{-6}
318	117.2	0.6389	1.34×10^{-4}	2.06×10^{-6}	1.65×10^{-5}	2.18×10^{-6}
318	133.8	0.7007	2.02×10^{-4}	4.18×10^{-6}	1.96×10^{-5}	1.35×10^{-5}
318	156.9	0.7518	2.64×10^{-4}	9.14×10^{-6}	2.32×10^{-5}	4.62×10^{-7}
318	187.5	0.7963	3.22×10^{-4}	1.12×10^{-5}	2.81×10^{-5}	6.00×10^{-7}
318	240.6	0.8479	3.51×10^{-4}	1.23×10^{-5}	3.01×10^{-5}	1.67×10^{-6}
328	133.4	0.5820	1.88×10^{-4}	1.05×10^{-5}	1.06×10^{-5}	1.03×10^{-6}
328	156.2	0.6684	2.93×10^{-4}	2.76×10^{-5}	1.73×10^{-5}	6.08×10^{-6}
328	169.6	0.6992	3.15×10^{-4}	2.46×10^{-5}	2.05×10^{-5}	1.58×10^{-6}
328	196.5	0.7465	3.93×10^{-4}	1.77×10^{-5}	2.54×10^{-5}	1.08×10^{-6}
328	236.5	0.7950	4.80×10^{-4}	1.28×10^{-5}	3.08×10^{-5}	1.21×10^{-6}

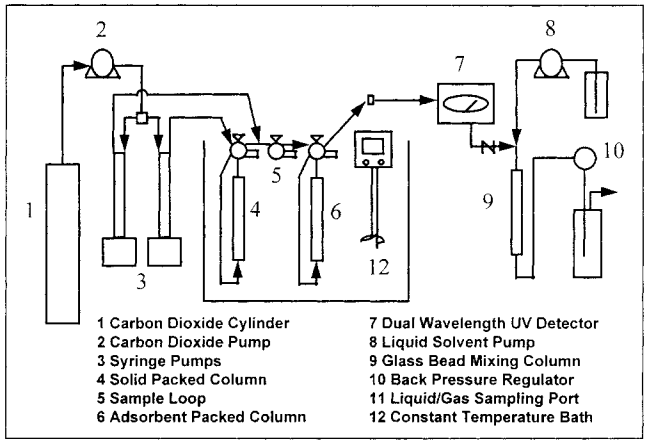

Figure 3. Experimental assembly for supercritical adsorption measurements.

concentration of the effluent samples in the supercritical fluid is calculated using the known supercritical fluid-flow rate, liquid solvent flow rate, and solute concentration in the liquid solvent. As shown by the simplified experimental setup (Figure 4), the measured response (E^*) in the solvent stream may be skewed from the actual response at the column effluent (E) due to mixing and system dispersion caused by the addition of the liquid stream. In addition, the adsorber response will be delayed by the residence time the fluid takes to flow between the UV detector at the column exit (point 2) and the separator (point 3). At this stage, the experimentalist has two options: to develop a hydrodynamic model which converts the mixing cup reading response in the alcohol stream (E^*) to the real response (E), or to determine the operating conditions at which negligible system dispersion is introduced in the two-fluid mixing region. In this study, the latter option was used. To test for negligible system dispersion or to calibrate a signal response model, adsorption breakthrough curve data taken for a single adsorbate were utilized. By measuring single component HCB adsorption breakthrough curves at both point 2 (the UV detector) and point 3 (the mixing cup), the additional system dispersion can be determined. If the response at point 3, corrected for residence time, coincides with the response at point 2, then the dispersion caused by the addition of the organic solvent into the system is negligible at that operating condition (Figure 4). We have determined that, at pressures above 1,700 psia and temperatures at or below 45°C, the dispersion due to the mixing section is negligible. Thus, the data measured at point 3 by mixing cup readings, corrected for residence time, represent the true column response and have dispersion due to adsorption, diffusion, mass transfer, and column hydrodynamics. In all the data presented, system dispersion tests were taken prior to any isotherm measurement to verify the above assumption.

Using the experimental apparatus, two isotherms were determined, one at 1,700 psia and 318 K and the second at 2,700 psia and 308 K using the calcium montmorillonite (average size of 5 μm) packed column. The measured column dimensions, supercritical fluid flow rate, bed and particle porosities, and average particle size for the set of experiments at 1,700 psia and 318 K are provided in Table 2. Be-

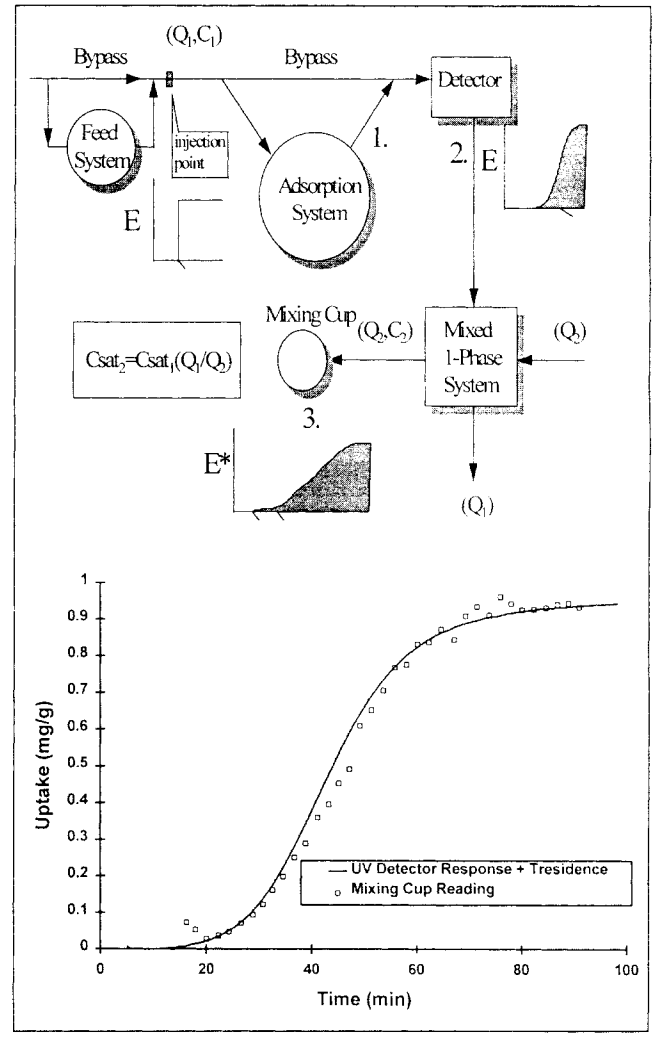

Figure 4. Experimental setup and dispersion comparison at the column exit and sampling point.

fore running any experiment, the packed column was first cleaned by passing pure supercritical carbon dioxide over the bed at the experimental conditions. Column breakthrough curves were then obtained in three individual experiments using series inlet loadings of 10%, 20%, and 30%, or 20%, 40%, and 60% saturated mixture streams to determine the adsorption isotherms at each condition. In all these cases a saturated supercritical fluid stream from the saturator (that is, a stream that has concentrations of HCB and PCP at the mixture solubility limit at the operating conditions) is mixed with a pure supercritical fluid stream to obtain the desired concentration level. It is important to note that at 20% concentration level, for example, the concentration of each species is 20% of its mixture solubility at the operating conditions. To series load a column at 20%, 40%, and 60%, the column is first loaded using a 20% saturated stream until the total breakthrough of both of the components is obtained. The feed stream is then increased to a 40% saturated mixture stream to obtain another set of breakthroughs for each component and continued in this manner up to the 60% loading. A typical set of series loading breakthrough curves is provided in Figure 5. Referring to this figure, the mass adsorbed at the

Table 2. Particle and Column Parameters for Experiments at 318 K and 1,700 psia (11.7 MPa)

Column Parameter	Value Measured
Mass Packing (g)	
Experiment 1	2.4110
Experiment 2	2.8003
Experiment 3	2.4260
Column diameter (cm)	0.7034
Supercrit. flow rate at 22°C (mL/h)	
Experiment 1	50
Experiment 2	100
Experiment 3	50
Avg. particle size (μm)	5.0
Particle porosity	0.31
Bed porosity	0.465
Particle density (g/mL)	1.875
BET surface area (m^2/g)	84.969

20% concentration level is then the area beneath the dimensionless concentration of 1.0 which lies to the left of each of the breakthrough curves. For the 40% loading, the mass adsorbed is that of the 20% loading plus the area to the left of the 40% breakthrough curve, between dimensionless concentrations of 1 and 2. A good separation between the two component fronts of PCP and HCB was obtained. Hexachlorobenzene was eluted first, while pentachlorophenol shows a much larger retention time in the column.

Using the series loading data, multicomponent Langmuir equations (Eqs. 12a and 12b) were fit to the two measured isotherms at each condition

$$q_1 = \frac{a_1 C_1}{1 + b_1 C_1 + b_2 C_2} \tag{12a}$$

$$q_2 = \frac{a_2 C_2}{1 + b_1 C_1 + b_2 C_2} \tag{12b}$$

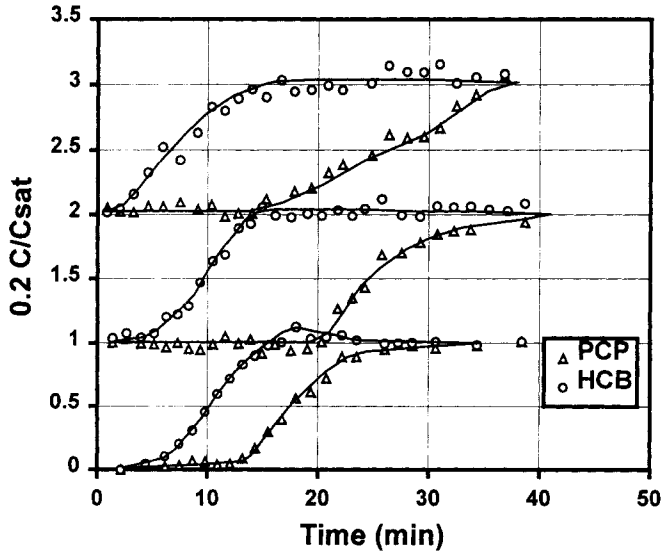

Figure 5. Series loading experiments at $T = 308$ K and $P = 2{,}700$ psia (11.7 MPa).

Table 3. Multicomponent Langmuir Isotherm Parameters

Langmuir Parameters	Calculated Value
at 318 K and 1,700 psia 1 .7 MPa	
a_1 (PCP) (mg/g × mol/L)	5,386.0
a_2 (HCB) (mg/g × mol/L)	2,278.6
b_1 (PCP) (mol/L)	610.5
b_2 (HCB) (mol/L)	808.2
at 308 K and 2,700 psia 8 .6 MPa	
a_1 (PCP) (mg/g × mol/L)	2,068.5
a_2 (HCB) (mg/g × mol/L)	877.2
b_1 (PCP) (mol/L)	109.5
b_2 (HCB) (mol/L)	−242.6

A multivariable parameter regression for a_1, a_2, b_1, and b_2 for the two isotherms (HCB and PCP) simultaneously was then performed using the entire data set collected at each condition. Langmuir adsorption constants at both conditions are provided in Table 3.

Model Results

The prediction of the breakthrough profiles was performed by employing Eqs. 1–7 with the empirically determined adsorption isotherms (Eq. 12 and Table 3) and inlet conditions given by mixture solubilities at the specified dilution level (Table 1). The remaining unknown hydrodynamic parameters were given order of magnitude values for prediction of the breakthrough curve to indicate how well such a model might describe a supercritical process. Predictions were initially made for the data at 318 K and 1,700 psia (11.7 MPa). Values used for the various parameters were initially derived from correlations available in the literature for supercritical carbon dioxide. Catchpole et al.'s (1996) correlation was used for prediction of the axial dispersion coefficient. Lee and Holder's (1995) correlation was used for prediction of the solid/fluid film mass-transfer coefficient, and Eaton and Akgerman's (1997) correlation for molecular diffusivity was combined with the Satterfield et al. (1973) expression for effective diffusivity using a tortuosity value of five. It should be noted that the molecular diffusion coefficients predicted by the Eaton-Akgerman equation and used to calculate the effective diffusivities are single component, infinite dilution diffusivities. This is, at best, an approximation for the multicomponent diffusivities, which truly define the system. However, in absence of data and any prediction techniques for multicomponent diffusion in supercritical fluids, we have used the single component values. The following order of magnitude values were used: 1.0×10^{-11} m^2/s for effective diffusivity of both components, 1.0×10^{-7} m^2/s for axial dispersion, and 1.0×10^{-3} m/s for film mass transfer. Through simulations, it was determined that these parameters, given by correlations alone, did not yield correct trends representative of the data measured, resulting in significantly steeper breakthrough profiles than represented by the experimental data. To identify which of the predicted parameters were out of range, pulse response experiments (which are described later) were performed to determine the system parameters. Moment analysis outlined by Schneider and Smith (1968) was utilized to yield estimates of axial dispersion and effective diffusivities, similar to that of the previous work in supercritical fluids

(Erkey and Akgerman, 1990). By comparing film mass-transfer resistance terms to diffusional resistance terms, mass-transfer contributions were found to be significantly small and considered negligible. This indicates that the controlling parameters involved with the column model are the effective diffusivity, axial dispersion, and multicomponent adsorption isotherms. As justified later, effective diffusivities measured using pulse chromatography corresponded well to those predicted. The axial dispersion coefficient measured, however, was on the order of 10^{-5} m^2/s, significantly higher than that predicted by the Catchpole et al. correlation. Figure 6 shows the prediction of the breakthrough profile at 318 K and 1,700 psia (11.7 MPa) using axial dispersion coefficients of 1×10^{-4}–1×10^{-6} m^2/s. At high dispersion coefficient values, the profiles were flatter indicating no frontal roll-up, whereas when dispersion coefficient is small, very sharp breakthrough profiles with a significant roll-up effect are observed in prediction. Comparison with the experimental data indicates that the axial dispersion values should be somewhere between 1×10^{-5} and 1×10^{-6} m^2/s indicating that the experimentally determined values by pulse chromatography were more realistic. To determine actual values, axial dispersion coefficients for the experiments at 1,700 psia (11.7 MPa) and 318 K at two different flow rates were fit using the column model. Since these experiments were taken at the same temperature and pressure, effective diffusivity was held constant. By operating at different flow rates, however, the breakthrough profiles should be different, and this difference should be a direct effect of the axial dispersion magnitude. Thus, a model which can describe the supercritical adsorption system should be able to predict the various profiles by changes in this one parameter only.

Figures 7 and 8 show the model predictions for experiments at 318 K and 1,700 psia (11.7 MPa) using two different flow rates of 50 mL/h and 100 mL/h, respectively. The resulting model predictions of the breakthrough curves for the experiment at 50 mL/h using the original parameter estimates given previously and an axial dispersion coefficient of 3.0×10^{-6} m^2/s predict the correct breakthrough times for

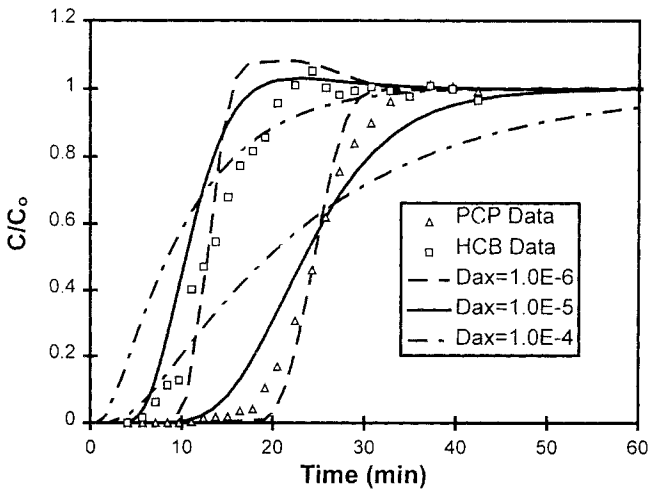

Figure 6. Adsorption breakthrough model prediction of the 20% saturated inlet stream at 1,700 psia (11.7 MPa) and 318 K with flow rate of 50 mL/h using different axial dispersion coefficients.

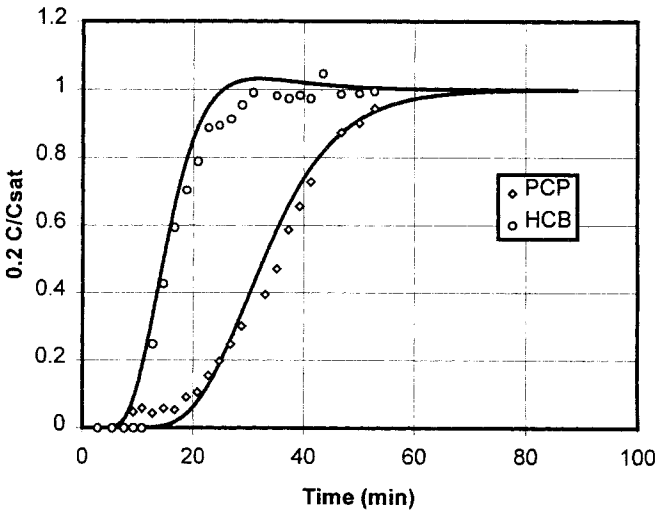

Figure 7. Adsorption breakthrough model prediction of the 20% saturated inlet stream at 1,700 psia (11.7 MPa) and 318 K with flow rate of 50 mL/h using an axial dispersion coefficient of 3×10^{-6} m^2/s.

both components measured. The predictions also have the correct trends represented by the data, although the model does predict a slight roll-up for HCB which is not clearly indicated by the data. This could be caused by slight errors in the breakthrough curve measurement and/or by errors due to using single component effective diffusivity values. For the model predictions at the same conditions, but with a 100 mL/h flow rate, a dispersion coefficient of 5×10^{-5} m^2/s was obtained from the data. Overall, the prediction of breakthrough curves using the model shows very good agreement with the measured data at both flow rates, by only adjusting the axial dispersion parameter.

Catchpole et al. (1996) model predicts that at very small particle sizes of around 5 μm, the axial dispersion is not a strong function of temperature and pressure, although their equation predicts values around 10^{-7} m^2/s at essentially all supercritical conditions listed. We made use of their observa-

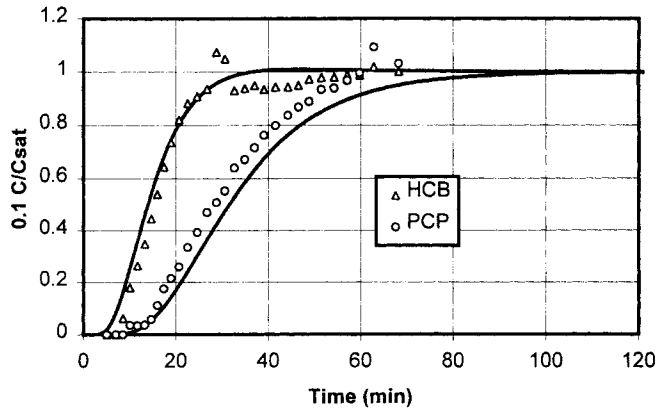

Figure 8. Adsorption breakthrough model prediction of the 10% saturated inlet stream at 1,700 psia (11.7 MPa) and 318 K with flow rate of 100 mL/h using an axial dispersion coefficient of 5×10^{-5} m^2/s.

tion and measured breakthrough curves at a new operating condition (different temperature and pressure) using the same interstitial velocity and compared model predictions utilizing the previously correlated values of axial dispersion to investigate how well the model can predict the new breakthrough curves without any additional parameter fitting. The comparison was made at 2,700 psia (18.6 MPa) and 308 K. The lower temperature and higher pressure produced a significant density difference of 0.639 g/cm^3 at 318 K and 1,700 psia (11.7 MPa) compared to 0.852 g/cm^3 at 308 K and 2,700 psia (18.6 MPa). The only remaining information required for the new prediction is the adsorption isotherms at this condition (also given in Table 3).

Results of the model predictions at the new condition using the same axial dispersion coefficient are given in Figure 9. The experimental data, as well as the model, show a slight roll-up. Model predictions, however, tend to occur slightly earlier for hexachlorobenzene with a smaller roll-up, which may be a direct effect of the limited amount of data used to describe the isotherm and use of pure component infinite dilution diffusivities rather than the multicomponent diffusivities. For this lower temperature and higher-pressure experiment, the breakthrough occurs considerably faster than that at the 318 K and 1,700 psia (11.7 MPa) condition. Again, the breakthrough prediction agrees very well with the measured data, given the new adsorption isotherms, showing that the model itself can be used to make predictions at other operating conditions which aid in finding conditions at which separation breakthrough curves may be optimized.

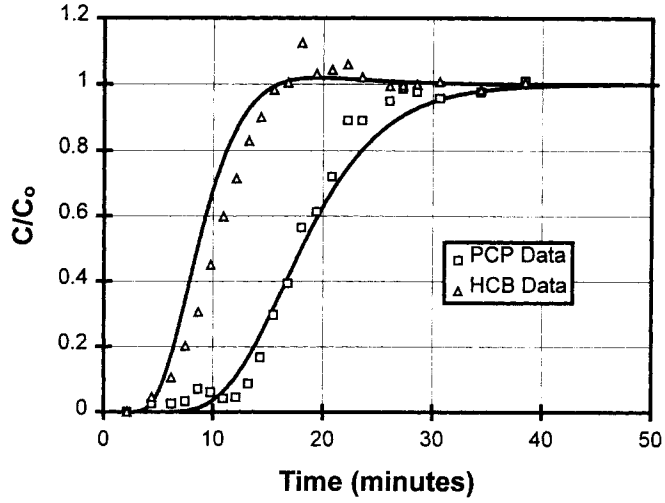

Figure 9. Adsorption breakthrough model prediction of the 20% saturated inlet stream at 2,700 psia (18.6 MPa) and 308 K with flow rate of 50 mL/h using an axial dispersion coefficient of 3×10^{-6} m^2/s.

Pulse Experiments for Separation Optimization

Given a column model which is robust enough to handle different supercritical conditions, the operating conditions for optimum separation can be determined. We have shown how this can be accomplished by coupling pulse chromatography with frontal analysis chromatography, identifying feed stream changes, and incorporating a new stability marker, partial molar volume.

In order to investigate how a supercritical separation like the one outlined may be optimized, moment analysis may be applied to determine which factors affect the shape of the breakthrough profile and how these factors change with temperature and pressure. For this particular analysis, a supercritical adsorptive system made up of a column and a two-phase solid particle, consisting of adsorbent solid and supercritical pore fluid, is considered. For the case of first-order reversible adsorption

$$\frac{\partial q}{\partial t} = k_a\left(C_P - \frac{q}{K_A}\right) \tag{13}$$

the analytical technique proposed by Schneider and Smith (1968) may be applied to yield the equations for the first and second moments. Application of the first and second central moments for determination of adsorber parameter for single component injections has been applied in numerous publications (Erkey and Akgerman, 1990; Uddin et al., 1990). Its extension into multicomponent pulse chromatography, however, requires additional assumptions which must be justified. If single component adsorption is treated as Langmuir type adsorption as shown by Eq. 14

$$A + S \underset{k}{\overset{k'}{\rightleftharpoons}} AS$$

$$\text{rate} = kC_AC_S - k'C_{AS}$$

$$q = C_{AS}$$

$$C_{S_{\text{total}}} = C_S + C_{AS} = q^\infty$$

$$K_{eq} = \frac{k}{k'}$$

$$\text{rate} = \frac{\partial q}{\partial t} = k\left[C_A(q^\infty - q) - \frac{q}{K_{eq}}\right] \tag{14}$$

this rate equation reduces to Eq. 13, reversible linear adsorption isotherm, only if $q \ll q^\infty$, that is, the number of sites available for adsorption are much more than the adsorbed amount of A. The extension of Langmuir type adsorption to the binary case

$$A + S \underset{k_a}{\overset{k'_a}{\rightleftharpoons}} AS$$

$$B + S \underset{k_b}{\overset{k'_b}{\rightleftharpoons}} BS$$

$$\text{rate}_1 = k_aC_AC_S - k'_aC_{AS}$$

$$\text{rate}_2 = k_bC_BC_S - k'_bC_{BS}$$

$$q_A = C_{AS}$$

$$q_B = C_{BS}$$

$$C_{S_{\text{total}}} = C_S + C_{AS} + C_{BS} = q^\infty$$

$$K_A = \frac{k_a}{k'_a}$$

$$\text{rate} = \frac{\partial q_A}{\partial t} = k_a\left[C_A(q^\infty - q_A - q_B) - \frac{q_A}{K_a}\right] \tag{15}$$

requires that the amount of adsorbed solute A and B combined would be negligible compared to the total number of sites available. This assumption essentially lumps the adsorption rate constant and site concentration into one constant k in Eq. 13.

If this assumption is valid, single component pulse injections can be used instead of multicomponent injection experiments for analysis of moments for a separation process since the linear isotherm functionality does not itself indicate dependence on the second component. This, unfortunately, is not the case in general since the rate constant and equilibrium constant themselves most often are functions of the second component. Such equilibrium effects, identified as displacement effects, have been discussed in the literature, and give rise to why multicomponent injections must be made instead of single component injections to obtain the correct linear rate (initial slope of the adsorption isotherm) and equilibrium constants (Gu et al., 1990). The moment analysis described earlier (Erkey and Akgerman, 1990) may then be applied to both component peaks of mixture injections individually.

The first absolute and second central moments of the pulse response yield the adsorption equilibrium constant, as well as dispersion coefficient and effective diffusivities (Schneider and Smith, 1968; Erkey and Akgerman, 1990). Using a pulse response apparatus similar to Figure 4, the effect of pressure and temperature on the adsorption parameters was studied. Temperature for the pulse separation of PCP and HCB experiments ranged from 308 K to 328 K, and pressures varied from a low of 1,700 psia (11.7 MPa) to a high of 2,700 psia (18.6 MPa). These conditions encompass a wide variety of carbon dioxide densities in the range 0.44 to 0.85 g/cm^3. The flow rate on the chromatography unit was run as high as possible, falling into the constant D_{ax}/U_i criterion (Erkey and Akgerman, 1990) yet low enough to allow for complete separation of the individual components, and causing negligible pressure drop [< 50 psi (345 kPa)]. To use a UV detector for analysis, complete separation of the two components is required. A small bore, 12-in. (305-mm)-long column with an OD of 0.25 in. (6.25 mm) and a wall thickness of 0.065 in. (1.651 mm) was used to record the desired separation results at a single wavelength of 240 nm.

Adsorption equilibrium constants for both HCB and PCP at three different pressures and temperatures are tabulated in Table 4. It has been shown that the adsorption equilibrium constant relates back to the capacity factor k, often used in chromatography work, through the expression given in Eq. 16 and is also provided in Table 4

$$k = \frac{(1-\epsilon_B)\rho_p K_A}{(1-\epsilon_B)\epsilon_p + \epsilon_B} \tag{16}$$

The capacity factor k for an individual component directly relates to the partial molar volume of that component in the mobile supercritical phase through Eq. 17 (Kelly and Chimowitz, 1990; Shim and Johnston, 1991)

$$\left(\frac{\partial \ln k}{\partial \ln \rho}\right)_T = -\left(1 - \frac{\overline{V_i^1}}{RTk_T}\right) \tag{17}$$

Table 4. Values of Adsorption Equilibrium Constant and Capacity Factor from First Moments

P (psia)	Temp. (K)	1st Moment	Ka	Capacity Factor
Hexachlorobenzene Pulse Response Results				
1,700	308	5.906	2.068568	3.367781
1,700	318	8.726	3.349548	5.453312
1,700	328	12.226	4.939417	8.041736
2,000	308	5.0086	1.660925	2.704109
2,000	318	6.0033	2.112766	3.43974
2,000	328	8.7855	3.376576	5.497315
2,700	308	4.8353	1.582204	2.575945
2,700	318	5.2503	1.770717	2.882859
2,700	328	5.9334	2.081014	3.388045
Pentachlorophenol Pulse Response Results				
1,700	308	73.271	32.66901	53.18756
2,000	308	77.335	34.51507	56.19309
2,000	318	107.37	48.15842	78.40547
2,700	308	48.056	21.21513	34.53981
2,700	318	53.06	23.48819	38.24051
2,700	328	66.082	29.40341	47.87093

SI conversion: MPa = psi × 0.00689

Given an equation of state, which describes the solute species in the supercritical fluid, the partial molar volume in the mobile phase can then be calculated along with the variation of K_A (the initial slope of the isotherm with density). Kelly and Chimowitz in 1990 built on this and described the variation of the capacity factor with respect to both temperature and pressure (Eqs. 18 and 19). In these equations, m represents the mobile phase (supercritical phase), s represents the stationary phase (the adsorbent or solid phase), β_m represents the isothermal compressibility, and θ represents the fractional coverage

$$\left(\frac{\partial \ln k}{\partial T}\right)_{P,y_j} = \left[\frac{\left(h_b^o - \bar{h}_b^m\right) + \Delta H_b^{ADS}}{RT^2}\right] + \alpha_m \tag{18}$$

$$\left(\frac{\partial \ln k}{\partial P}\right)_{T,y_b} = (1-\theta_b)\frac{\overline{h_b^m} - \overline{V_b^s}}{RT} - \theta_a \frac{\overline{V_a^m} - \overline{V_a^s}}{RT} - \beta_m \tag{19}$$

Knowing how the capacity factor varies with temperature, the variation of capacity factor with density at constant pressure can be calculated using Eq. 20 with an equation of state

$$\left(\frac{\partial \ln k}{\partial \ln \rho}\right)_{P,y_b} = \left(\frac{\partial \ln k}{\partial T}\right)_{P,y_b}\left(\frac{\partial T}{\partial V}\right)_{P,y_b} \tag{20}$$

Using the Peng-Robinson EOS and Wong-Sandler mixing rules, we calculated the partial molar volumes and partial molar enthalpies of the two components (Cross and Akgerman, 1997). Experimental and calculated data for the partial molar volumes were found to correspond well for PCP. The heats of adsorption (provided in Table 5) were then back calculated knowing the variation of capacity factor with temperature at constant pressure and constant mole fraction of the carrier.

Unlike gases, supercritical fluid adsorption capacity factors taken at constant pressure increase with increasing temperature up to a point. At high temperatures, the density effect

Table 5. Heats of Adsorption

Solute	Pres. psia	Temp. K	h_i^m kJ/mol	ΔH_i^{ADS} kJ/mol	Alpha kJ/mol	dk/dT	ΔH_i^{ADS} kcal/mol
HCB	1,700	350	−31	−17	14	0	−4.06
PCP	1,700	350	−54.7	−40.7	14	0	−9.72
HCB	2,700	365	−26	−17	9	0	−4.06
PCP	2,700	365	−44	−35	9	0	−8.36

SI conversion: MPa = psi × 0.00689

eventually causes decreases in the capacity factor. This implies the existence of a maximum for the amount adsorbed at a given pressure. The Kelly and Chimowitz lattice model is utilized to predict this point, and with this information the heats of adsorption are calculated. Following this routine, the capacity factor variation with temperature was modeled by making a best fit of the only adjustable lattice model parameter, the solute well depth to Boltzman constant ratio. By comparing calculated capacity factor values with the measured values, the ratios of well depth to Boltzman's constant for HCB and PCP were determined as −7,600 and −10,000, respectively. These values compare well on an order of magnitude level with those of the previous study on naphthalene, 2,3 dimethylnaphthalene, and 2,6 dimethylnaphthalene, ranging around −12,000 (Kelly and Chimowitz, 1990). Figure 10 shows capacity factor data and prediction for HCB; similar results were obtained for PCP (Cross, Jr., 1997). Table 5 gives the calculated heats of adsorption using Eq. 19 for the two different pressures. The average heat of adsorption value for PCP was calculated as 9.04 kcal/mol (37.85 kJ/mol), a little over twice that of HCB. The capacity factor of PCP was much greater than that of HCB, as expected. The capacity factors for both components are higher at lower pressures, which corresponds to the measured results. In order to have an increase in the capacity factor with temperature, the partial molar enthalpy component must become significantly large in comparison to the heat of adsorption and the volume expansivity (d_m). This only occurs at high temperatures and relatively low pressures in the supercritical regime.

Feed Stream and Stability Considerations

Given knowledge of the profiles for the capacity factor (or the adsorption equilibrium), if one was to try now to achieve better separations, it may seem feasible at first to operate at higher temperatures (around 350 K) and lower pressures [near or below 1,700 psia (11.7 MPa)]. Although such analysis may work well for pulse separations, the direct extension to frontal analysis can be misleading because of two important factors.

The first is the effect of such a condition on the feed stream concentration. As the temperature increases at low pressures, the solubility of the components often decreases due to the falling supercritical fluid density. Feed stream optimization, that is, the inlet concentrations of the species (having the upper limit as the mixture solubility), therefore conflict with the optimum for adsorption equilibrium.

To illustrate this point, we compare the measured isotherms at the two operation conditions used for the montmorillonite experiments, 308 K with 2,700 psia (18.6 MPa) and 318 K with 1,700 psia (11.7 MPa). Figure 11 shows both measured isotherms for PCP. The amount of PCP adsorbed at the higher temperature and low pressure is actually less than that at the high pressure and low temperature. Although this result may seem to conflict with theory by Kelly and Chimowitz, this is not the case due to the changes in mixture solubility at the different conditions. What Eqs. 18 and 19 provide is the variation of equilibrium constant with temperature and pressure for a noninteracting solute system; however, this does not relate to the mass adsorbed at each condition. Rather, it relates to the ratio of solute concentration on the adsorbent compared to that in the solvent. Whether this ratio is 11:1 or 6:1 depends on the type of purity values required for a particular product. Although this is of some interest, it has only limited use in frontal analysis chromatography since the main

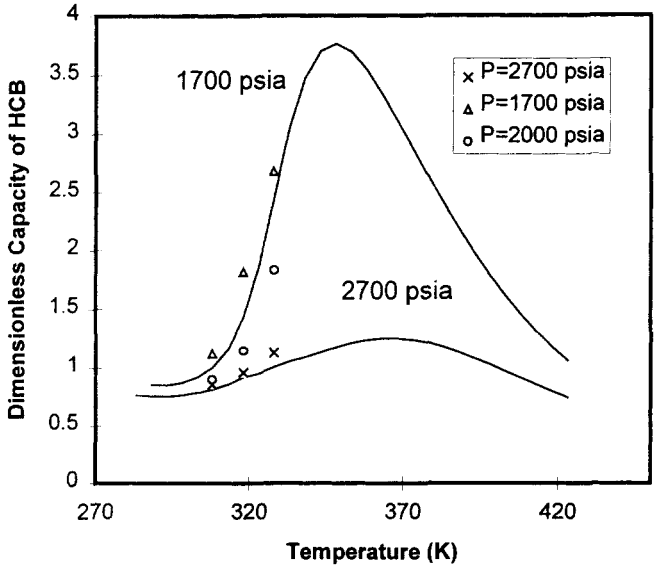

Figure 10. HCB capacity factor, data and model prediction.

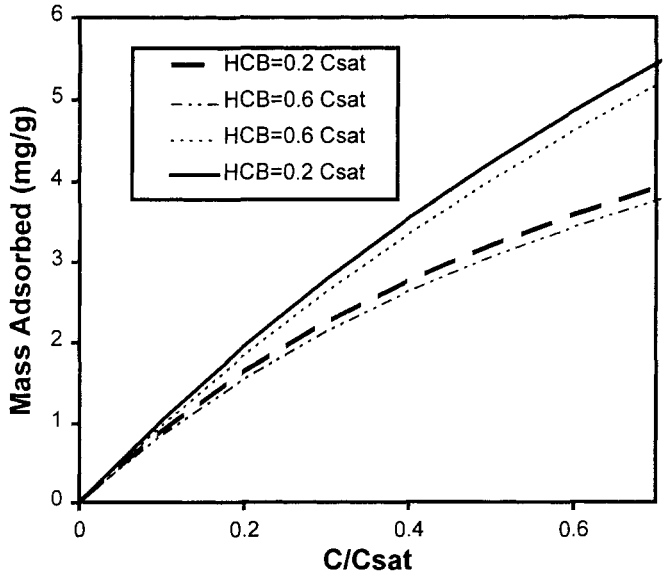

Figure 11. Adsorption isotherms for PCP in presence of constant HCB concentration.

Upper curves at 308 K; lower curves at 318 K.

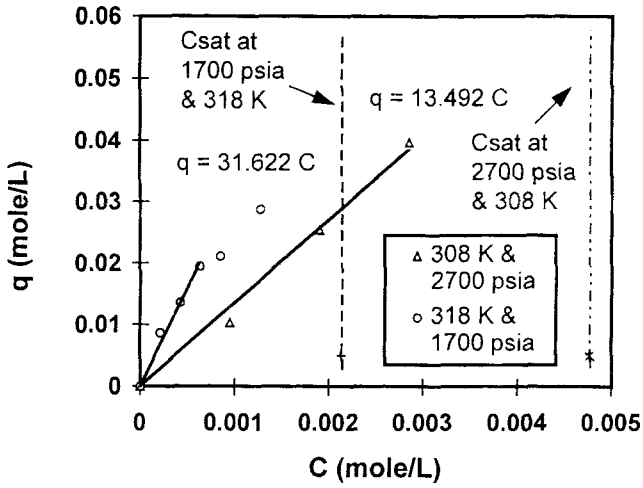

Figure 12. Equilibrium partitioning of PCP at 318 K and 1,700 psia (11.7 MPa) and at 308 K and 2,700 psia (18.6 MPa).

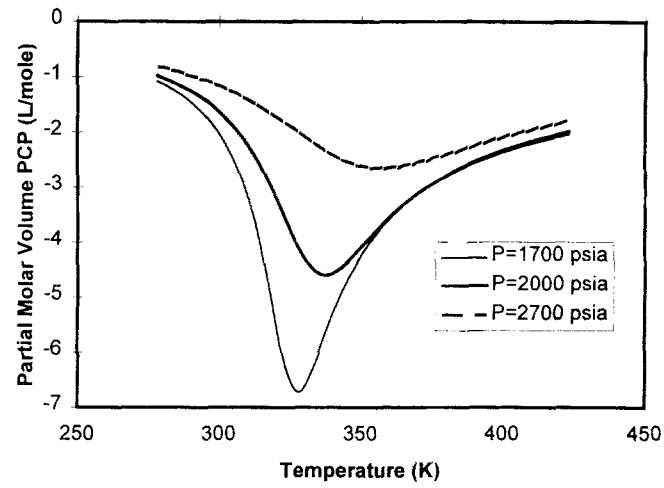

Figure 13. Partial molar volume of PCP.

concern, beyond this ratio alone, is maximizing the difference between total masses of each component adsorbed. To clearly see these differences, Figure 12 was developed to show the amount of adsorbed PCP with respect to its concentration in the supercritical phase. As predicted, the equilibrium constant, given by the initial slope in Figure 12, is larger for the higher temperature and lower pressure, however, the adsorbent material holds less solute mass per gram of solid adsorbent at this condition, and the amount adsorbed can be much higher at low temperature and high pressure.

A second factor, which is not obvious, is that of system stability. When dealing with supercritical systems, the pressure and temperature range considered for process operation becomes very important because as conditions are modified such that they start to approach the critical point, large variations in chemical properties occur. To relate stability of a supercritical system, a marker is needed. One of the most useful stability markers for pure gases is the isothermal compressibility, which provides practical insight on how a liquid or gas is behaving, either highly compressible or almost incompressible. For systems such as reactors or adsorbers, where the feed stream concentration for two or more components is the main point of interest, a more useful marker is

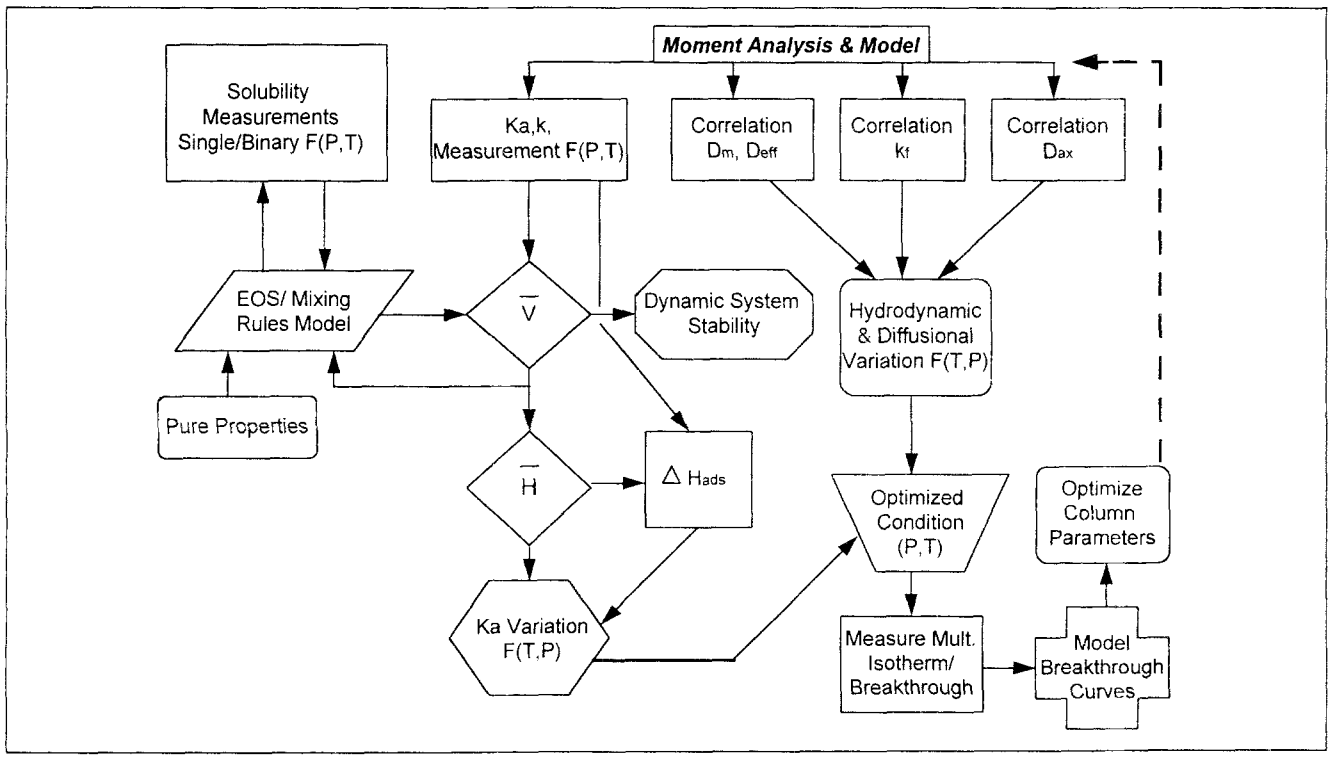

Figure 14. Road map to optimization of supercritical adsorptive separation.

the partial molar volume. Partial molar volume relates directly to the isothermal compressibility, but it also correlates to the feed composition. Partial molar volume for mixtures changes tremendously as one approaches the critical point (approaching negative infinity). Figure 13 gives the partial molar volumes of PCP at different conditions. The system would be inherently more unstable at 1,700 psia (11.7 MPa) due to large negative partial molar volumes. In fact our experimental system was impossible to operate with a stable effluent response at 318 K and 1,700 psia pressure (hence, no data reported at that condition). This large instability was introduced due to slight pulsation caused by expansion system and feed pump. With an appropriate equation of state and proper mixing rules at various supercritical conditions, it is possible to approximate how stable the inlet concentrations will be with respect to small variations in system pressure caused by a pump or compressor.

Conclusion

We have developed a new experimental technique to accurately measure multicomponent adsorption isotherms and solubilities of heavy molecular weight components in supercritical fluids using frontal analysis chromatography. A model separation of PCP/HCB was successfully performed at laboratory scale, indicating the potential of supercritical fluid adsorptive processes for separation of structurally similar compounds, such as pharmaceuticals and other human consumables of similar structure. The multicomponent adsorption isotherms for the model system were determined directly from the breakthrough curves and used to make theoretical model predictions for several breakthrough profiles at a variety of pressures, temperatures, and flow rates. For parameters which are not yet well correlated, like axial dispersion, it was also shown that pulse chromatography techniques can be applied to directly measure hydrodynamic and transport properties present in an adsorption system.

Incorporation of a multicomponent column model was found to be an important extension to fundamental understanding of which hydrodynamic and transports processes control the process and how these may be adjusted to yield better separations. By only measuring the isotherms and using previously correlated hydrodynamic parameters, breakthrough curves at new conditions could be predicted, extending the model's usefulness.

To conclude, we propose a decision map, such as given in Figure 14, which may be followed to produce a column model and separation process which yield more optimized multicomponent breakthrough profiles while lowering processing costs. This map starts with determination of an EOS for the prediction of solubilities, partial molar volumes, and partial molar enthalpies to yield predictions of adsorption equilibrium changes, system stability, and feed stream conditions. It ends with final column model parameter identification using pulse response analysis, parameter correlations, and column model tuning based on measured breakthrough profiles.

Notation

Bi_i = Biot number for species i in the bulk phase, $[(k_{f_i} R_P)/D_{e_i}]$
C_i = concentration of species i in the bulk phase, mol/m^3
C_i^s = concentration of species i at the surface of the particle, mol/m^3
C_{pi} = concentration of species i in the particle pore fluid, mol/m^3
D_{ax} = axial dispersion coefficient, m^2/s
D_{ei} = effective diffusivity of species i, m^2/s
$\overline{h}_i^j$ = partial molar enthalpy of species i in phase j
k_a = adsorption rate constant
k_f = film mass-transfer coefficient, m/s
k_T = isothermal compressibility, 1/bar
L = length of bed, m
Pe_B = bulk phase Peclet number, $L\nu/D_{ax}$
Pe_{Pi} = particle phase Peclet number for species i, $(R_p \nu/D_{e_i})$
q_i = solid phase concentration (amount adsorbed) of species i, mg/g
R = gas constant
R_p = radius of a particle, m
$\overline{V}_i^j$ = partial molar volume of species i in phase j
z = dimensionless length, x/L
α_m = volume expansivity
ϵ_B = bed porosity
ϵ_P = particle porosity
ρ = dimensionless particle radius, r/R_p
τ = dimensionless time, $t\nu/L$

Literature Cited

Bruno, T. J., and J. F. Ely, *Supercritical Fluid Technology: Reviews in Modern Theory and Applications*, CRC Press, Boca Raton, FL (1991).

Catchpole, O. J., R. Bering, and M. B. King, "Measurement and Correlation of Packed-Bed Axial Dispersion Coefficients in Supercritical Carbon Dioxide," *Ind. Eng. Chem. Res.*, **35**, 824 (1996).

Chihara, K., M. Suzuki, and K. Kawazoe, "Adsorption Rate on Molecular Sieving Carbon by Chromatography," *AIChE J.*, **24**, 237 (1978).

Cross, Jr., W. M., "Adsorptive Separations by Supercritical Frontal Analysis Chromatography," PhD Diss., Texas A&M Univ. (1997).

Cross, Jr., W. M., C. Erkey, and A. Akgerman, "Determination of Chelate Complex Solubilities in Supercritical Fluids," *Ind. Eng. Chem. Res.*, **35**, 1123 (1996).

Cross, W., and A. Akgerman, "Single Component and Mixture Solubilities of Hexachlorobenzene and Pentachlorophenol in Supercritical Carbon Dioxide," *Ind. Eng. Chem. Res.*, **39**, 1510 (1997).

Eaton, A. P., and A. Akgerman, "Infinite Dilute Diffusion Coefficients in Supercritical Fluids," *Ind. Eng. Chem. Res.*, **36**, 923 (1997).

Erkey, C., G. Madras, M. Orejuela, and A. Akgerman, "Supercritical Carbon Dioxide Extraction of Organics from Soil," *Environ. Sci. Technol.*, **27**, 1225 (1993).

Erkey, C., and A. Akgerman, "Chromatography Theory: Application to Supercritical Extraction," *AIChE J.*, **36**, 1715 (1990).

Gu, T., G. T. Tsao, G.-J. Tsai, and M. R. Landish, "Displacement Effect of Multicomponent Chromatography," *AIChE J.*, **36**, 8 (1990).

Kelly, F. D., and E. H. Chimowitz, "Near-Critical Phenomena and Resolution in Supercritical Fluid Chromatography," *AIChE J.*, **36**, 1163 (1990).

Lee, C. H., and G. Holder, "Use of Supercritical Fluid Chromatography for Obtaining Mass Transfer Coefficients in Fluid-Solid Systems at Supercritical Conditions," *Ind. End. Chem. Res.*, **34**, 906 (1995).

Lin, W. F., and C. S. Tan, "Separation of M-Xylene and Ethylbenzene on Silicalite," *Sep. Sci. Technol.*, **26**, 1549 (1991).

Macnaughton, S., and N. Foster, "Supercritical Adsorption and Desorption Behavior of DDT on Activated Carbon Using Carbon Dioxide," *Ind. Eng. Chem. Res.*, **34**, 275 (1995).

Madras, G. C., C. Erkey, and A. Akgerman, "Supercritical Fluid Regeneration of Activated Carbon Loaded with Heavy Molecular Weight Organics," *Ind. Eng. Chem. Res.*, **32**, 1163 (1993).

Madras, G. C., C. Thibaud, C. Erkey, and A. Akgerman, "Modeling of Supercritical Extraction of Organics from Solid Matrices," *AIChE J.*, **40**, 777 (1994).

Modell, M., and R. C. Reid, *Thermodynamics and Its Applications*, International Series in Physical and Chemical Engineering Sciences, Prentice-Hall, Englewood Cliffs, NJ (1983).

Mullins, J. A., J. B. Rawlings, and K. P. Johnston, "Partial Derivative Quantities from Phase Equilibria Relationship for Mixtures," *AIChE J.*, **39**, 1363 (1993).

Ruthven, D. M., *Principles of Adsorption and Adsorption Processes*, Wiley, New York (1984).
Sakanishi, K., H. Obata, I. Mochida, and T. Sakaki, "Capture and Recovery of Indole from Methylnaphthalene Oil in a Continuous Supercritical CO_2 Extraction Apparatus over a Fixed Bed of Anion-Exchange Resin," *Ind. Eng. Chem. Res.*, **35**, 335 (1996).
Santacesaria, E., M. Morbidelli, A. Servida, S. Giuseppe, and S. Carra, "Separation of Xylenes on Y Zeolites. 2. Breakthrough Curves and Their Interpretation," *Ind. Eng. Chem. Process Des. Dev.*, **21**, 446 (1982).
Satterfield, C. N., C. K. Colton, and W. H. Pitcher, "Restricted Diffusions in Liquids within Fine Pores," *AIChE J.*, **19**, 628 (1973).
Schneider, P., and J. M. Smith, "Chromatographic Study of Surface Diffusion," *AIChE J.*, **14**, 886 (1968).
Shim, J.-J., and K. P. Johnston, "Phase Equilibria, Partial Molar Enthalpies, and Partial Molar Volumes Determined by Supercritical Fluid Chromatography," *J. Phys. Chemistry*, **95**, 353 (1991).
Svarovsky, L., ed., *Solid-Liquid Separation*, Butterworths, London (1990).
Tan, C.-S., and D.-C. Liou, "Axial Dispersion of Supercritical Carbon Dioxide in Packed Beds," *Ind. Eng. Chem. Res.*, **28**, 1246 (1989).
Tan, C. S., and J. L. Tsay, "Separation of Xylene Isomers on Silicalite in Supercritical and Gaseous Carbon Dioxide," *Ind. Eng. Chem. Res.*, **29**, 502 (1990).
Uchida, H., Y. Iwai, A. Amiya, and Y. Arai, "Adsorption Behaviors of 2,6- and 2,7-Dimethylnaphthalenes in Supercritical Carbon Dioxide Using NaY-Type Zeolite," *Ind. Eng. Chem. Res.*, **36**, 424 (1997).
Uddin, M. S., K. Hidajat, and C. Ching, "Liquid Chromatographic Evaluation of Equilibrium and Kinetic Parameters of Large Amino Acids on Silica Gel," *Ind. Eng. Chem. Res.*, **29**, 647 (1990).
Yu, Q., and N. H. L. Wang, "Computer Simulations of the Dynamics of Multicomponent Ion Exchange and Adsorption in Fixed Beds—Gradient-Directed Moving Finite Element Method," *Computer Chem. Eng.*, **13**, 915 (1989).

Manuscript received Oct. 17, 1997, and revision received Apr. 22, 1998.